Single-frequency Dielectric Model of Frozen Mineral Soils for Frequencies of the Basic Satellites

V. L. Mironov[1], S. V. Fomin[1], Y. I. Lukin[1],
A. Y. Karavaysky[1], and I. P. Molostov[2]

[1]Kirensky Institute of Physics, SB RAS, Russia
[2]Altai State University, Russia

Abstract— A simple single-frequency dielectric model for the set of frequencies which are 0.45, 1.26, 1.4, 1.6, 5.4, 6.9, 9.6, and 10.7 GHz for frozen mineral soils is developed. The model is based on the dielectric measurements of three typical soils (sandy loam, silt loam, and silty clay) at the temperature range from $-1°C$ to $-30°C$. The measured data as a function of moisture were fitted with the refractive mixing dielectric model. The model parameters are maximum bound water fraction, and refractive indexes of soil solid, unfrozen bound water, and wet ice. In the result of fitting measured data, the model parameters were determined as a functions of soil type (clay content), and soil temperature. The error of the predicted values of the complex relative permittivity (CRP) of frozen soils relative to the measured ones was evaluated through determination coefficients, and root mean square error (RMSE). The values of RMSE are on the order of the dielectric measurement error itself. The proposed dielectric model can be applied in active and passive remote sensing techniques used in the cold regions.

1. INTRODUCTION

Soil moisture, temperature, freez/thaw (F/T) state impact the water and energy cycles and the exchange of greenhouse gases between land and atmosphere. Dielectric models of topsoil are a crucial element of remote sensing retrieval algorithms that are used to obtain geophysical characteristics of the land surface [1, 2]. For positive temperatures there is a sufficient number of models such as the spectroscopic dielectric models for 1.4–18 GHz [3], and 45 MHz–26.5 GHz [4], and single frequencies dielectric models for 1.4 GHz, 5 GHz [5], 1.4 GHz [6], which are used in the algorithms of the soils moisture retrieval. As for the frozen mineral soils, in the literature there are a very limited number of the dielectric constant measurements [7], and the dielectric model is only one model [8] that is purely theoretical and has not been verified in experimental data.

The aim of this paper is to develop a simple dielectric model of frozen mineral soils on separate frequencies commonly used in remote sensing. Most of the existing microwave sensors operate at the frequencies of 1.26 GHz (ALOS PALSAR), 1.4 GHz (SMOS, SMAP), 1.6 GHz (GPS), 5.4 GHz (SENTINEL1), 9.6 GHz (TerraSAR-x, 6.9 and 10.7 GHz (GCOM-W1, AMSR-E), which only sense soil surface moisture (0–5 cm depth). It is promising the creation of such a model at a frequency of 450 MHz, in course of the recent NASA "Airborne Microwave Observatory of Subcanopy and Subsurface" (AirMOSS) mission provides an unprecedented sensing depth of about 50 cm to directly retrieve root zone soil moisture under vegetation canopies [9]. The model is based on dielectric measurements of the Arctic mineral soils with different texture in the range of moisture changes from zero to full moisture saturation, with positive and negative temperatures at MHz and GHz frequency bands.

2. EXPEREMENTAL DATA

To develop the dielectric model we measured the three basic soils collected in Yamal, Russia (soils 1, 2, 3 in Table 1). As seen from Table 1, mineral compositions of the basic soils are rather close to each other, though, their textures in term of clay content vary in the range from 9.1 to 41.3%. Dielectric measurements for frozen soils were carried out in the frequency range from 0.45 to 15 GHz for the soil moistures from zero to field capacity, when the temperature changes from $-1°C$ to $-30°C$.

Before measuring, the soil samples were dried in an oven at $104°C$ for 6 hours. To obtain samples with moisture, a different quantities of distilled water were added into soil samples by calibrated pipette. The prepared samples were mixed well and then were stored in a sealed container at least for one day. To conduct dielectric measurement, the soil sample was placed into a cell formed by a section of coaxial waveguide with the cross section of 7/3 mm (Fig. 1), the latter ensuring that

Table 1. The soil texture parameters and mineral composition.

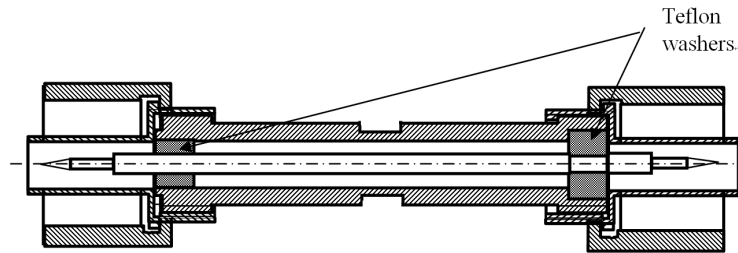| No.	Soil Type	Soil Texture (%)			Mineral Composition				
		Sand	Silt	Clay	Quartz (%)	Feldspar (%)	Plagioclase (%)	Mica, chlorite (small impurity)	Smectite, Amphibol, Siderite (traces)
1	Sandy loam	41.4	49.5	9.1	40	30	30	Imp	Tr
2	Silt loam	40.4	39.0	20.6	70	15	5–10	Imp	Tr
3	Silty clay	1.6	57.1	41.3	60	20–25	5	Imp	Tr

Figure 1. The drawing of the measuring cell.

only TEM mode is present in the measured frequency range. The length of sample placed in the cell and its volume were equal to $17\,\mathrm{mm}$ and $0.529\,\mathrm{cm^3}$, respectively.

When filling the measuring cell, the soil was compacted with a cylinder pestle. The cell was blocked on both sides with teflon washers, which prevented the sample from changing in volume. The measuring cell was connected to the ZVK Rohde&Schwarz or Agilent vector network analyzers to measure the frequency spectra of the S_{11}, S_{22}, S_{12}, and S_{21} elements of the scattering matrix S over the frequency range from $45\,\mathrm{MHz}$ to $15\,\mathrm{GHz}$. The isothermal measurements were ensured with the use of an SU-241 Espec chamber of heat and cold with accuracy $0.5°\mathrm{C}$. The algorithm developed in [10] was applied to retrieve the spectra of the complex relative permittivity (CRP) of moist sample using the measured values of S_{11} and S_{12} or S_{22} and S_{21}. This algorithm provides the real and imaginary parts of the CRP of moist samples with the errors less than 10% and 20%, respectively. The example of measured data are presented in Fig. 2.
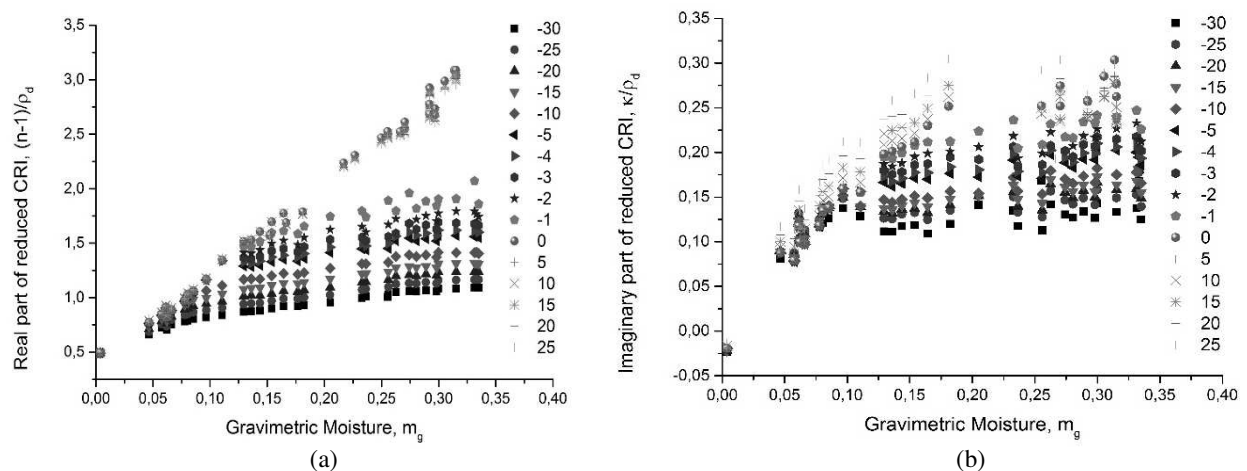

Figure 2. The reduced complex refractive index (CRI) as a function of gravimetric moisture for the soil 3 (see Table 1) at different temperatures (from $-30°\mathrm{C}$ to $25°\mathrm{C}$). (a) The real part of reduced CRI, (b) the imaginary part of reduced CRI.

The measured data are shown in terms of the reduced complex refractive index (CRI). CRI depending on moisture have the form of piecewise linear functions, and their easier were fitted. The values of CRI, $n^* = n + i\kappa$, and complex relative permittivity (CRP), $\varepsilon^*\varepsilon' + i\varepsilon''$, are linked to

each other by the following equations:

$$\varepsilon' = n^2 - \kappa^2, \quad \varepsilon'' = 2n\kappa. \tag{1}$$

Due to experimenter unequal forces when he was filling the soil samples and that it is impossible to compress moistened soil strongly, density of the soil samples varied considerably in the measuring process, in the range of 5–20% (Table 2).

Table 2. Soil samples gravimetric moistures, m_g [g/g], and their respective soil densities, ρ_d [g/cm^3].

Soil 1	m_g	0.004	0.005	0.012	0.023	0.039	0.047	0.052	0.061	0.072	0.091	0.097	0.101	0.117
	ρ_d	1.617	1.6	1.652	1.539	1.478	1.507	1.525	1.552	1.492	1.529	1.547	1.57	1.575
	m_g	0.135	0.155	0.156	0.159	0.165	0.182							
	ρ_d	1.648	1.79	1.861	1.785	1.672	1.651							
Soil 2	m_g	0.003	0.025	0.04	0.042	0.058	0.064	0.064	0.066	0.068	0.071	0.093	0.111	0.132
	ρ_d	1.516	1.363	1.411	1.399	1.29	1.36	1.335	1.673	1.365	1.339	1.426	1.441	1.454
	m_g	0.138	0.143	0.149	0.154	0.171	0.18	0.192	0.209	0.211				
	ρ_d	1.504	1.552	1.714	1.455	1.827	1.478	1.803	1.632	1.615				
Soil 3	m_g	0.004	0.047	0.058	0.061	0.062	0.066	0.078	0.08	0.085	0.097	0.111	0.129	0.136
	ρ_d	1.296	1.398	1.323	1.339	1.329	1.283	1.361	1.359	1.376	1.398	1.476	1.571	1.443
	m_g	0.144	0.154	0.164	0.177	0.182	0.205	0.233	0.236	0.256	0.263	0.274	0.28	0.289
	ρ_d	1.492	1.481	1.541	1.514	1.551	1.593	1.595	1.629	1.576	1.539	1.516	1.502	1.488
	m_g	0.298	0.3	0.315	0.331	0.333	0.335							
	ρ_d	1.439	1.456	1.423	1.386	1.338	1.381							

In order to neutralize this effect in the process of a model construction we fitted the reduced CRI, $(n-1)/\rho_d$ and κ/ρ_d. Here ρ_d is the density of dry soil. Looking at the measured data, we can say that the values of the real part of CRI (Fig. 2(a)) for frozen soil samples ($T \leq -1$) varies greatly depending on temperature compared to thawed soil samples ($T \geq 0$). While the values of imaginary part of CRI variation depending on the temperature for thawed soil samples are comparable to those of the frozen soil.

3. DIELECTRIC MODEL

At Fig. 3 measured data for three soils with different texture are shown as a function ofgravimetric moisture at fixed temperature ($-1°$C) and fixed electromagnetic frequency (450 MHz). It can be seen that each of the three sets of data has a single kink (m_{g1}) and the two different area of reduced CRI changing. In the first area ($m_g \leq m_{g1}$) values of real and imaginary parts of CRI grow faster than those in the second area ($m_g \geq m_{g1}$). The value m_{g1} we call the maximum of bound water fraction (MBWF). In the first area the soil samples contain only unfrozen bound water, in the second region the soil samples contain an unfrozen bound water and wet ice. These measured data were fitted with the refractive mixing dielectric model as formulated in [11]:

$$\frac{n_s - 1}{\rho_d} = \begin{cases} \frac{n_m-1}{\rho_m} + \frac{n_b-1}{\rho_b}m_g & m_g \leq m_{g1} \\ \frac{n_m-1}{\rho_m} + \frac{n_b-1}{\rho_b}m_{g1} + \frac{n_i-1}{\rho_i}(m_g - m_{g1}) & m_g > m_{g1} \end{cases} \tag{2}$$

$$\frac{\kappa_s}{\rho_d} = \begin{cases} \frac{\kappa_m}{\rho_m} + \frac{\kappa_b}{\rho_b}m_g & m_g \leq m_{g1} \\ \frac{\kappa_m}{\rho_m} + \frac{\kappa_b}{\rho_b}m_{g1} + \frac{\kappa_i}{\rho_i}(m_g - m_{g1}) & m_g > m_{g1} \end{cases} \tag{3}$$

The subscripts s, d, m, b, and i (which are related to n, κ, and ρ) refer to the moist soil, dry soil, mineral component of soil, unfrozen bound water, and wet ice, respectively.

The measured data sets as a function of soil moisture at a fixed temperature and frequency, as shown in Fig. 3, were fitted by the piecewise linear functions (2) and (3), using the software ORIGIN 9.0. When fitting measured data for three types of soil simultaneously we have made the following assumptions. The reduced CRI's of mineral component ($(n_m - 1)/\rho_m$ and κ_m/ρ_m), unfrozen bound water ($(n_b - 1)/\rho_b$ and κ_b/ρ_b), and wet ice ($(n_i - 1)/\rho_i$ and κ_i/ρ_i) of soils depend only on temperature, and do not depend on soil texture. The maximum gravimetric fractions of the unfrozen bound water, m_{g1}, depends on both texture and temperature of soil. As a result,
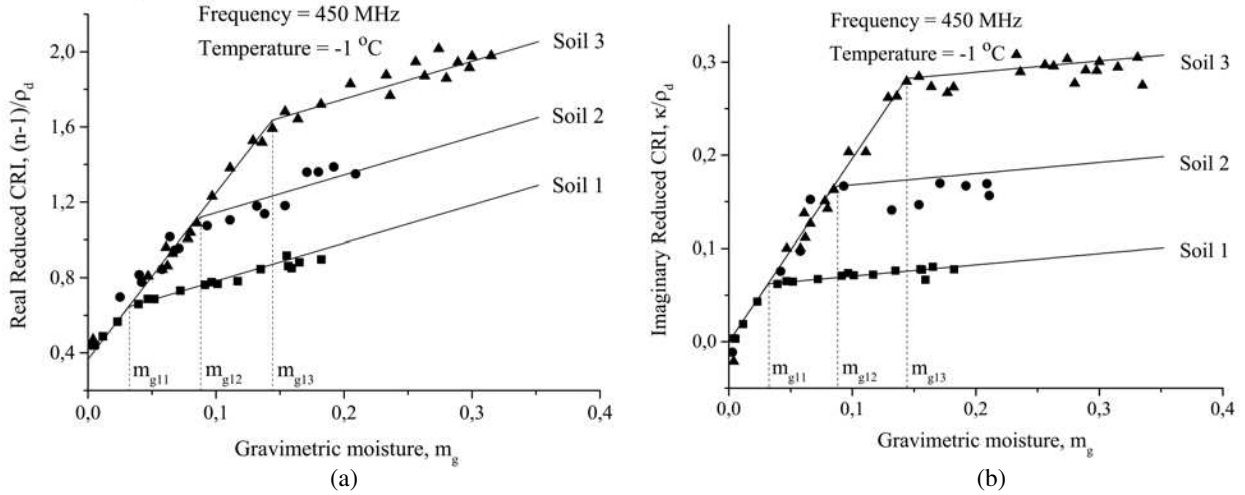
Figure 3. The reduced complex refractive index of the measured soils (symbols) as a function of gravimetric moisture. (a) The real part of the reduced CRI, (b) the imaginary part of the reduced CRI.

there were derived 1) the MBWF, m_{g11}, m_{g12}, and m_{g13}, pertaining to the soils 1, 2, and 3 (see Table 1), 2) the reduced CRIs for the bound water, $(n_b - 1)/\rho_b$, κ_b/ρ_b, wet ice, $(n_i - 1)/\rho i$, κ_i/ρ_i, and mineral part of soil, $(n_m - 1)/\rho_m$, κ_m/ρ_m, which were considered to be the same for all three soils. The above fitting procedure was repeated for the measured data obtained at the temperatures of -1, -2, -1, -2, -3, -5, -10, -15, -20, -25, $-30°C$, yielding the reduced CRI parameters $(n_m - 1)/\rho_m$, $(n_b - 1)/\rho_b$, $(n_i - 1)/\rho_i$, κ_m/ρ_m, κ_b/ρ_b, and κ_i/ρ_i as a function of temperature. While the values of MBWF, m_{g1}, were derived with the applied fitting procedure as a function of both the temperature and percentage of clay content $Clay$, that is, m_{g1} $(T, Clay)$, which is shown in Fig. 4.

Below, there are presented the dielectric model parameters as a function of soil temperature and texture. The coefficients A, B, and C are shown in Table 3.

$$
\begin{aligned}
m_{g1} &= A \cdot Clay \cdot (1 + B \cdot \exp(T/C)) \\
(n_m - 1)/\rho_m &= A + B \cdot \exp(T/C) \\
(n_b - 1)/\rho_b &= A + B \cdot T + C \cdot T^2 \\
(n_i - 1)/\rho_i &= A + B \cdot \exp(T/C) \\
\kappa_m/\rho_m &= 0 \\
\kappa_b/\rho_b &= A + B \cdot T + C \cdot T^2 \\
\kappa_i/\rho_i &= A + B \cdot T + C \cdot T^2
\end{aligned}
\tag{4}
$$

Equations (1)–(4) represent the temperature and texture dependent dielectric model for the CRP of frozen mineral soils at the one frequency. To calculate the CRP for one of the proposed frequency as a function of gravimetric moisture or as a function of temperature using formulas in (1)–(4), one must assign the following variables: 1) dry soil density, ρ_d [g/cm^3], 2) gravimetric moisture, m_g [g/g], 3) temperature, $T°C$, and 4) clay content in soil, $Clay$ in %.

4. VALIDATION OF THE DIELECTRIC MODEL

The results of the measurements for the soil 1, and 3 (see Table 1) are shown in Fig. 5 as a function of temperature, together with the respective predictions obtained with the use of the formulas in (1)–(4). As seen from Fig. 5, the calculated data are in good agreement with the measured ones.

To quantify the developed model error, we correlated the predicted CRPs with the set of measured CRPs relating to three soils with different moistures in the entire region of the measured temperature. In Fig. 6, the predicted values of the real part (Fig. 6(a)) and the imaginary part (Fig. 6(b)) of the CRP are presented versus the respective measured values. To estimate the error, we calculated the coefficient of determination for the real, R_ε^2, and the imaginary, R_ε^2, parts of the CRP, and root mean square errors (RMSEs) based on the data like shown in Fig. 6. Accuracy of the model predictions are presented in Table 4.
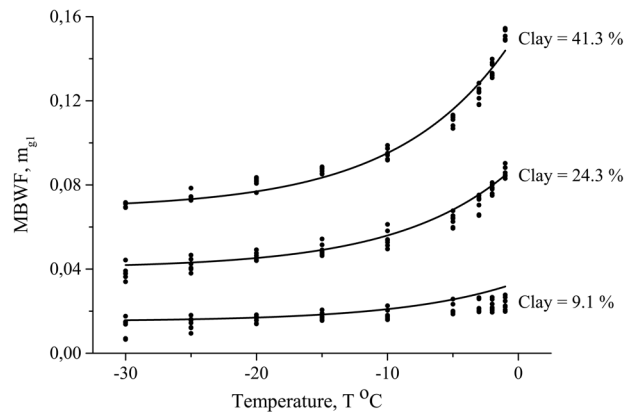
Figure 4. The MBWF as a function of temperature for individual soils. The symbols represent the results of fittings obtained with the data like those given in Fig. 3 and the model given by (2) and (3). The solid lines correspond to the fits as given by the first equation in (4).

Table 3. Coefficients of functional dependences for the model parameters.

|	F (GHz)	0.45	1.26	1.4	1.6	5.4	6.9	9.6	10.7
m_{gl}	A	0.00166							
	B	1.232							
	C	8.633							
$(n_m\text{-}1)/\rho_m$	A	0.424	0.401	0.405	0.413	0.407	0.417	0.414	0.417
	B	-0.0967	-0.0676	-0.0686	-0.0695	-0.0739	-0.0779	-0.0648	-0.0601
	C	1.911	1.808	1.907	1.729	2.220	2.90398	2.437	2.760
$(n_b\text{-}1)/\rho_b$	A	8.455	8.231	8.098	7.902	6.961	6.571	5.907	5.690
	B	0.091	0.0842	0.0883	0.0927	0.159	0.171	0.151	0.147
	C	0.00053	0	0	0	0.00177	0.00213	0.00206	0.00207
$(n_i\text{-}1)/\rho_i$	A	1.418	1.424	1.428	1.384	1.211	1.222	1.204	1.201
	B	0.976	0.954	0.862	0.921	0.851	1.0562	0.741	0.732
	C	1.939	3.361	3.780	3.381	4.676	3.210	3.610	3.579
κ_b/ρ_b	A	2.0136	1.455	1.456	1.463	2.160	2.328	2.482	2.500
	B	0.0537	-0.0108	-0.0276	-0.0362	-0.0055	0.0232	0.0515	0.0510
	C	0.0012	-0.000257	-0.00058	-0.00076	-0.00119	-0.000559	0.000031	0
κ_i/ρ_i	A	0.114	0.129	0.1164	0.110	0.282	0.375	0.381	0.416
	B	-0.00655	-0.000735	-0.00397	-0.00695	0.0126	0.0238	0.0228	0.0264
	C	-0.000204	-8.29E-05	-0.00015	-0.00023	0.000219	0.00047	0.000399	0.000513

(a)

(b)
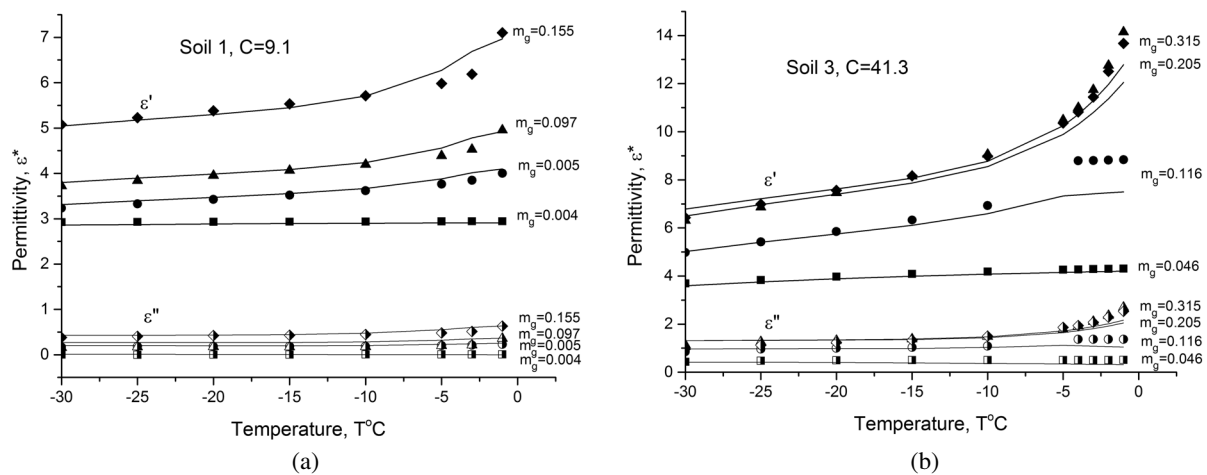
Figure 5. The CRP of moist soil as a function of temperature at the fixed gravimetric moistures m_g (given by inscriptions) and the frequency of 1.4 GHz. (a) Soil 1, clay content 9.1%. (b) Soil 2, clay content 41.3%. The measured CRP values are represented by symbols. The solid lines correspond to the CRPs estimated with the dielectric model (1)–(4).
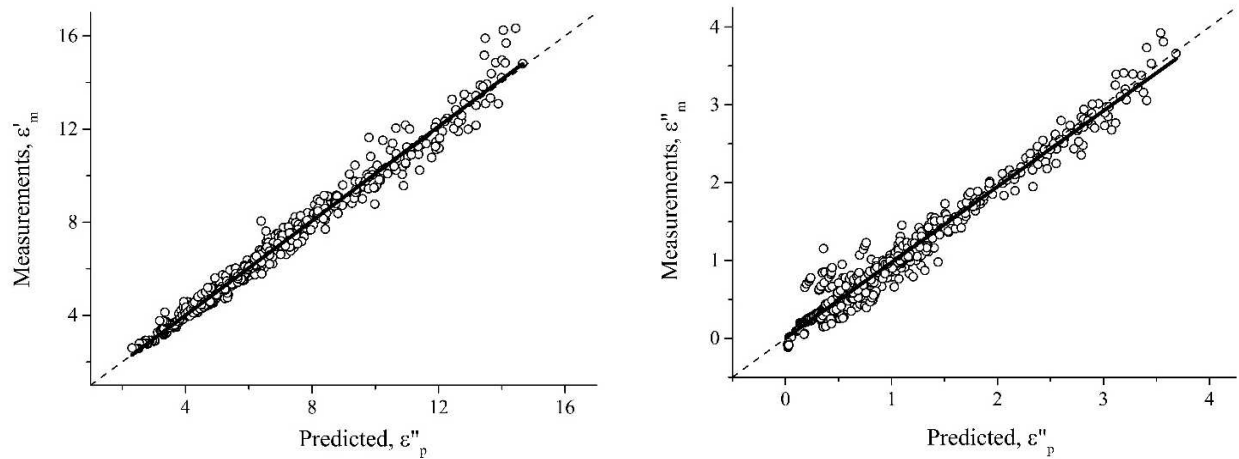
Figure 6. The calculated CRPs of moist soils as a function of the measured ones in the temperature ranges of $-30°C \leq T \leq -1°C$, for the frequency of 450 MHz. Bisectors represented by the dotted lines. Liner fits represented by the solid lines.

Table 4. Equations of linear regression, determination coefficients (R^2) and RMSE between measured and predicted values of CRP for frozen soils at different frequencies.

F, GHz	ε'			ε''		
	line equation	R^2	RMSE	line equation	R^2	RMSE
0.45	$\varepsilon'_m = -0.0438 + 1.0127 \cdot \varepsilon'_p$	0.982	0.384	$\varepsilon''_m = 0.0022 + 0.9735 \cdot \varepsilon''_p$	0.965	0.152
1.26	$\varepsilon'_m = -0.0320 + 1.0033 \cdot \varepsilon'_p$	0.988	0.310	$\varepsilon''_m = -0.0207 + 0.9626 \cdot \varepsilon''_p$	0.962	0.121
1.4	$\varepsilon'_m = -0.0299 + 1.0049 \cdot \varepsilon'_p$	0.987	0.315	$\varepsilon''_m = -0.0449 + 0.9618 \cdot \varepsilon''_p$	0.958	0.131
1.6	$\varepsilon'_m = -0.0875 + 1.0162 \cdot \varepsilon'_p$	0.985	0.326	$\varepsilon''_m = -0.0418 + 0.9483 \cdot \varepsilon''_p$	0.958	0.130
5.4	$\varepsilon'_m = -0.0924 + 1.0230 \cdot \varepsilon'_p$	0.985	0.266	$\varepsilon''_m = -0.0283 + 0.9878 \cdot \varepsilon''_p$	0.978	0.131
6.9	$\varepsilon'_m = -0.0613 + 1.0149 \cdot \varepsilon'_p$	0.987	0.233	$\varepsilon''_m = -0.0104 + 0.9695 \cdot \varepsilon''_p$	0.974	0.148
9.6	$\varepsilon'_m = -0.0795 + 1.0206 \cdot \varepsilon'_p$	0.987	0.203	$\varepsilon''_m = -0.0199 + 0.9692 \cdot \varepsilon''_p$	0.972	0.152
10.7	$\varepsilon'_m = -0.0737 + 1.0183 \cdot \varepsilon'_p$	0.988	0.187	$\varepsilon''_m = -0.0438 + 0.9659 \cdot \varepsilon''_p$	0.970	0.157

5. CONCLUSIONS

A temperature- and texture-dependent single-frequency dielectric model was developed for frozen mineral soils on the base of dielectric measurements of three soils with clay content 9.1%, 20.6%, and 41.3%. Soil texture is specified according to the American classification of soils. The model provides the CRPs of the frozen mineral soils as a function of dry soil density, moisture, texture (clay content), and temperature at the frequencies of 0.45, 1.26, 1.4 1.6, 5.4, 6.9, 9.6 10.7 GHz. The model was validated by the good agreement with the measured data. To calculate the CRP of frozen soil as a function of moisture and temperature using formulas in (1)–(4), we should know: 1) dry soil density, ρ_d [g/cm^3], and 2) clay content in soil, $C\%$. The developed dielectric model can be used in data processing algorithms for modern and future remote sensing missions.

REFERENCES

1. Mialon, A., P. Richaume, D. Leroux, S. Bircher, A. Al Bitar, T. Pellarin, J.-P. Wigneron, and Ya. H. Kerr, "Comparison of dobson and mironov dielectric models in the SMOS soil moisture retrieval algorithm," *IEEE Trans. Geosci. Remote Sens.*, Vol. 53, No. 6, 3084–3094, Jun. 2015.
2. Chan, S. K., R. Bindlish, P. E. O'Neill, et al., "Assessment of the SMAP passive soil moisture product," *IEEE Trans. Geosci. Remote Sens.*, Vol. 54, No. 8, 4994–5007, Aug. 2016.
3. Dobson, M. C., F. T. Ulaby, M. T. Hallikainen, and M. A. El-Rayes, "Microwave dielectric behavior of wet soil-Part II: Dielectric mixing models," *IEEE Trans. Geosci. Remote Sens.*, Vol. 23, No. 1, 35–46. 1985.

4. Mironov, V. L., L. G. Kosolapova, and S. V. Fomin, "Physically and mineralogically based spectroscopic dielectric model for moist soils," *IEEE Trans. Geosci. Remote Sens.*, Vol. 47, No. 7, Part 1, 2059–2070, Jul. 2009.

5. Wang, J. R. and T. J. Schmugge, "An empirical model for the complex dielectric permittivity of soils as a function of water content," *IEEE Trans. Geosci. Remote Sens.*, Vol. 18, No. 4, 288–295, 1980.

6. Mironov, V., Y. Kerr, J.-P. Wigneron, L. Kosolapova, and F. Demontoux, "Temperature and texture dependent dielectric model for moist soils at 1.4 GHz," *IEEE Geosc. Remote Sens. Letters*, Vol. 10, No. 3, 419–423, 2013.

7. Zhao, S., L. Zhang, Y. Zhang, and L. Jiang, "Microwave emission of soil freezing and thawing observed by a truck-mounted microwave radiometer," *International Journal of Remote Sensing*, Vol. 33, No. 3, 860–871, 2012.

8. Zhang, L., J. Shi, Z. Zhang, and K. Zhao, "The estimation of dielectric constant of frozen soil-water mixture at microwave bands," *Proc. of IGARSS*, 2903–2905, Toulouse, France, Jul. 21–25, 2003.

9. Tabatabaeenejad, A., M. Burgin, and M. Moghaddam, "P-band radar retrieval of subcanopy and subsurface soil moisture profile as a second order polynomial: First AirMOSS results," *IEEE Trans. Geosci. Remote Sens.*, Vol. 53, 645–658, 2015.

10. Mironov, V. L., I. P. Molostov, Y. I. Lukin, and A. Y. Karavaisky, "Method of retrieving permittivity from S_{12} element of the waveguide scattering matrix," *International Siberian Conference on Control and Communications (SIBCON)*, Krasnoyarsk, 978-1-4799-1062-5/13 ©2013 IEEE, Sep. 12–13, 2013,

11. Mironov, V. L., Ya. Kerr, L. G. Kosolapova, I. V. Savin, and K. V. Muzalevskiy, "Temperature dependent dielectric model for an organic soil thawed and frozen at 1.4 GHz," *IEEE J. Sel. Topics Appl. Earth Observ. Remote Sens. (JSTARS)*, Vol. 8, No. 9, 4470–4477, 2015.